AGU PUBLICATIONS

Paleoceanography

RESEARCH ARTICLE

10.1002/2017PA003178

Key Points:
- Agreement between solution phase ICP-MS and LA-ICP-MS shows the accuracy of using NIST 612 glass to measure bamboo coral Ba/Ca via LA-ICP-MS
- High intracoral reproducibility demonstrated in skeletal Ba/Ca records from eight bamboo coral calcite samples
- Interannual-decadal scale Ba/Ca variability in NE Pacific corals may provide insights into changes in intermediate ocean biogeochemistry

Supporting Information:
- Supporting Information S1
- Data Set S1

Correspondence to:
G. Serrato Marks,
gserrato@mit.edu

Citation:
Serrato Marks, G., M. LaVigne, T. M. Hill, W. Sauthoff, T. P. Guilderson, E. B. Roark, R. B. Dunbar, and T. J. Horner (2017), Reproducibility of Ba/Ca variations recorded by northeast Pacific bamboo corals, *Paleoceanography*, *32*, 966–979, doi:10.1002/2017PA003178.

Received 6 JUN 2017
Accepted 3 AUG 2017
Accepted article online 18 AUG 2017
Published online 13 SEP 2017

Reproducibility of Ba/Ca variations recorded by northeast Pacific bamboo corals

G. Serrato Marks[1], M. LaVigne[1], T. M. Hill[2], W. Sauthoff[2], T. P. Guilderson[3,4], E. B. Roark[5], R. B. Dunbar[6], and T. J. Horner[7]

[1]Earth and Oceanographic Science Department, Bowdoin College, Brunswick, Maine, USA, [2]Earth and Planetary Sciences Department, University of California, Davis, California, USA, [3]Department of Ocean Sciences, University of California, Santa Cruz, California, USA, [4]Center for Acceleration Mass Spectrometry, Lawrence Livermore National Laboratory, Livermore, California, USA, [5]Department of Geography, Texas A&M University, College Station, Texas, USA, [6]Department of Earth System Science, Stanford University, Stanford, California, USA, [7]Department of Marine Chemistry and Geochemistry, Woods Hole Oceanographic Institution, Woods Hole, Massachusetts, USA

Abstract Trace elemental ratios preserved in the calcitic skeleton of bamboo corals have been shown to serve as archives of past ocean conditions. The concentration of dissolved barium (Ba_{SW}), a bioactive nutrientlike element, is linked to biogeochemical processes such as the cycling and export of nutrients. Recent work has calibrated bamboo coral Ba/Ca, a new Ba_{SW} proxy, using corals spanning the oxygen minimum zone beneath the California Current System. However, it was previously unclear whether Ba/Ca_{coral} records were internally reproducible. Here we investigate the accuracy of using laser ablation inductively coupled plasma mass spectrometry for Ba/Ca_{coral} analyses and test the internal reproducibility of Ba/Ca among replicate radial transects in the calcite of nine bamboo corals collected from the Gulf of Alaska (643–720 m) and the California margin (870–2054 m). Data from replicate Ba/Ca transects were aligned using visible growth bands to account for nonconcentric growth; smoothed data were reproducible within ~4% for eight corals (n = 3 radii/coral). This intracoral reproducibility further validates using bamboo coral Ba/Ca for Ba_{SW} reconstructions. Sections of the Ba/Ca records that were potentially influenced by noncarbonate bound Ba phases occurred in regions where elevated Mg/Ca or Pb/Ca and coincided with anomalous regions on photomicrographs. After removing these regions of the records, increased Ba/Ca_{coral} variability was evident in corals between ~800 and 1500 m. These findings support additional proxy validation to understand Ba_{SW} variability on interannual timescales, which could lead to new insights into deep sea biogeochemistry over the past several centuries.

1. Introduction

The cycling of marine nutrients is linked to global climate through the biological carbon pump [e.g., *Roemmich and McGowan*, 1995; *Ainley and Hyrenbach*, 2010; *Deutsch et al.*, 2011; *McQuatters-Gollop et al.*, 2011]. However, high-resolution records of marine nutrient dynamics in the intermediate and deep ocean are relatively scarce because of challenges associated with repeat sampling and insufficient resolution of extant sedimentary archives. Cold-water corals provide a potentially powerful means to obtain such records of intermediate and deep ocean conditions due to their longevity and ubiquity within the ocean interior [e.g., *Adkins et al.*, 1998; *Heikoop et al.*, 2002; *Risk et al.*, 2002; *Anagnostou et al.*, 2011]. Moreover, certain types of deep-sea coral, such as bamboo corals (jointed gorgonian octocorals; family Isididae, order Alcyonacea), can provide archives of ambient and surface water conditions at interannual to decadal resolution [e.g., *Noe and Dullo*, 2006; *Thresher et al.*, 2009, 2010; *LaVigne et al.*, 2011; *Sinclair et al.*, 2011; *Hill et al.*, 2014; *Farmer et al.*, 2015a, 2015b; *Saenger and Watkins*, 2016; *Thresher et al.*, 2016]. As bamboo corals grow (~50–180 μm/yr), calcareous internodes and organic nodes are simultaneously precipitated using distinct carbon sources: proteinaceous nodes incorporate particulate organic carbon, whereas high-Mg calcite internodes incorporate ambient dissolved inorganic carbon [*Andrews et al.*, 2005; *Roark et al.*, 2005; *Noe and Dullo*, 2006; *Tracey et al.*, 2007; *Thresher et al.*, 2009; *Hill et al.*, 2011; *Frenkel et al.*, 2017]. As such, individual bamboo coral specimens have the potential to provide continuous interannual to decadal records of both ambient (intermediate or deep waters) and surface water conditions over several hundred years.

The geochemistry of the calcitic internodes of bamboo corals has been shown to reflect several properties of ambient seawater, such as temperature [*Thresher et al.*, 2010; *Hill et al.*, 2011; *Saenger and Watkins*, 2016;

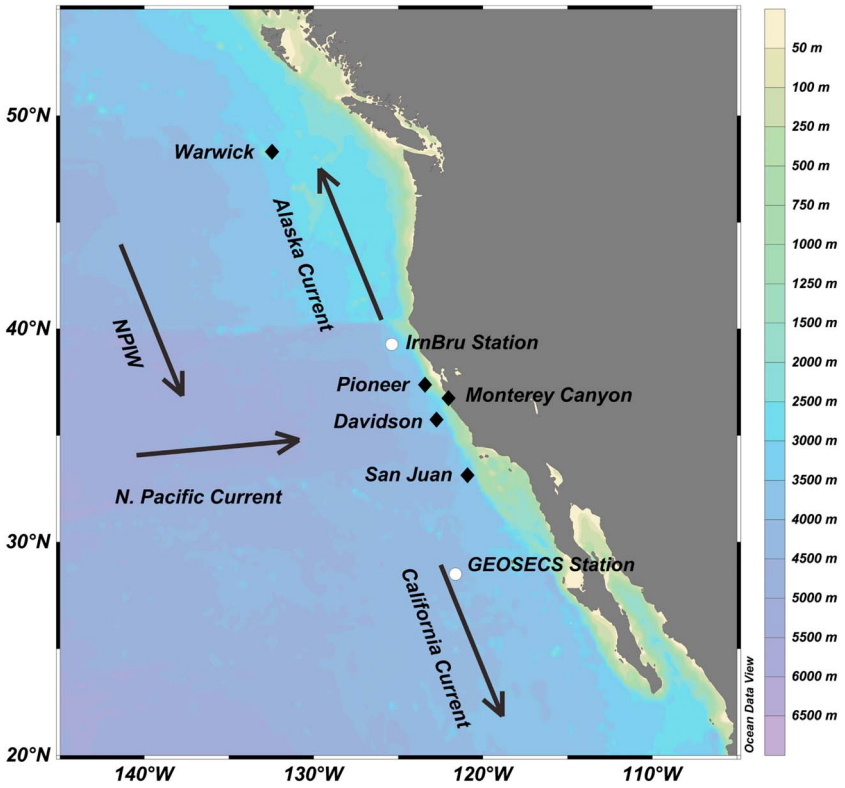

Figure 1. Bathymetric map of coral (black diamonds) and seawater (white circles) sample locations in the Gulf of Alaska and California margin. Arrows show California Current System circulation, adapted from *Howell et al.* [2012]. Map created with Ocean Data View [*Schlitzer*, 2016].

Thresher et al., 2016] and aspects of seawater chemistry [e.g., *Sinclair et al.*, 2011; *LaVigne et al.*, 2011; *Hill et al.*, 2012; *Raddatz et al.*, 2014; *Thresher et al.*, 2016]. Of the seawater chemistry properties, those that potentially reflect marine nutrients, such as dissolved barium (Ba_{SW}), are of particular interest as their cycling can be linked to the export and mineralization of organic carbon in the ocean interior [e.g., *Bishop*, 1988; *Dymond et al.*, 1992; *Esser and Volpe*, 2002; *Bishop and Wood*, 2008]. Specifically, calibrations based on the outermost growth bands of live-collected bamboo coral internodes showed that skeletal Ba/Ca ratios (Ba/Ca_{coral}) faithfully reflect ambient Ba_{SW} via lattice substitution of Ba for Ca [e.g., *LaVigne et al.*, 2011; *Thresher et al.*, 2016]. Despite this potential to record seawater nutrient histories, a study by *Sinclair et al.* [2011] remains the only investigation into the internal reproducibility of time-resolved Ba/Ca_{coral} variations. This lack of thorough validation currently hinders fully realizing the utility of the bamboo coral Ba/Ca proxy to reconstruct intermediate and deep ocean Ba_{SW}—and thus nutrient and carbon—chemistry through time.

In order to further evaluate the validity of the Ba/Ca_{coral} proxy, we test the internal reproducibility of Ba/Ca in nine deep-sea coral bamboo specimens across a depth transect in the northeast Pacific Ocean using LA-ICP-MS (laser ablation inductively-coupled plasma mass spectrometry). To evaluate the accuracy of the LA-ICP-MS measurements, we compare these data with pubished solution-based ICP-MS Ba/Ca_{coral} data from the outermost growth bands of the same corals. Finally, we examine these new profiles in the context of a new depth profile of dissolved Ba_{SW} collected nearby. With the notable exceptions of juvenile growth and non-carbonate intergrowths, our data suggest that bamboo coral Ba/Ca reflects northeast Pacific nutrient chemistry over the life spans of individual corals (~100 years) and hints at possible short-term biogeochemical changes in the eastern Pacific oxygen minimum zone (OMZ) within the last century.

2. Methods

2.1. Samples

The nine samples used in this study include two Gulf of Alaska corals and seven California margin corals, all of which have been described previously (Figure 1) [e.g., *Roark et al.*, 2005; *LaVigne et al.*, 2011; *Hill et al.*, 2012].

Table 1. Coral Samples Utilized in This Study

Sample	Depth (m)	Location	Seamount/Site	Taxonomy	Live/Dead	Age (Years) [*Roark et al.*, 2005]	Growth Rate (μm/yr)
ALV3808 #5	634	48.3N, 132.44W	Warwick	Isidae	Live	126 ± 8	160 ± 10[a]
ALV3808 #3	720	48.3N, 132.44W	Warwick	Isidae	Live	75 ± 5	120 ± 10[a]
T1104 A7	870	36.74N, 122.03W	Monterey Canyon	*Isidella*	Live	-	90[b]
T1101 A13	1012	37.37N, 123.41W	Pioneer	*Isidella*	Live	-	93[b]
T664 A17	1295	33.13N, 120.91W	San Juan	*Keratoisis*	Live	-	-
T1102 A12	1500	35.73N, 122.73W	Davidson	*Keratoisis*	Live	-	-
T1102 A10	1521	35.73N, 122.73W	Davidson	*Keratoisis*	Live	-	-
T664 A2	1954	33.15N, 120.89W	San Juan	*Lepidisis*	Live	-	70[a]
T664 A1	2055	33.15N, 120.89W	San Juan	*Isidella*	Live (dead at base)	-	72[a]

[a] *Roark et al.* [2005].
[b] *Hill et al.* [2014].

The location of the atmospheric ^{14}C bomb spike has been identified in the proteinaceous gorgonin nodes of six samples and used to estimate the radial extension rate and age of these specimens in previous studies (Table 1) [*Roark et al.*, 2005; *Hill et al.*, 2011, 2014; *Frenkel et al.*, 2017]. However, recent work has revealed evidence of growth rate nonlinearity in bamboo corals, limiting age model development for these specimens [*Roark et al.*, 2005; *Farmer et al.*, 2015b; *Frenkel et al.*, 2017]. The Gulf of Alaska corals were collected live from Warwick Seamount in 2002 using the DSV *Alvin* and stored at Stanford University [*Roark et al.*, 2005]. California margin samples were collected from Pioneer, San Juan, and Davidson Seamounts, as well as Monterey Canyon in 2004 and 2007 using the ROV *Tiburon* on the Monterey Bay Aquarium Research Institute (MBARI) R/V *Western Flyer* and archived at University of California (UC) Davis (Table 1). With the exception of T664A1, all specimens were living at the time of collection. The specimens were identified based on morphological characteristics as belonging to the *Isidella*, *Lepidisis*, and *Keratoisis* subfamilies (Table 1) [*Roark et al.*, 2005; *LaVigne et al.*, 2011; *Hill et al.*, 2012], though ongoing revisions to bamboo coral taxonomy raise the possibility that other related taxa are represented within our sample set [*France*, 2007; *LaVigne et al.*, 2011; *Hill et al.*, 2014].

2.2. Hydrographic Context

All samples were collected from within the north Pacific OMZ (Figure 2) spanning the Gulf of Alaska to the California margin. In this region, the North Pacific Current (NPC) flows from west to east between the subtropical and subpolar gyres (~35°N; Figure 1) [*Howell et al.*, 2012]. As it approaches the eastern boundary of the Pacific basin, the NPC splits into the north flowing Alaska current and the south flowing California Current. Beneath this Ekman-induced coastal upwelling zone, the California Current System (CCS) region exhibits a strong OMZ with intermediate to severe hypoxia (defined as O_2 = 22–61 μmol/kg or <22 μmol/kg, respectively) [*Karstensen et al.*, 2008; *Moffitt et al.*, 2015]. The California margin OMZ is influenced by well ventilated, low-salinity North Pacific Intermediate Water (potential density of 26.2–26.9 σ_θ) as well as low oxygen Antarctic Intermediate Water (potential density 26.9–27.6 σ_θ; Figure 2) [*Reid*, 1965; *Lynn and Simpson*, 1987; *Talley*, 2008; *Van Scoy and Druffel*, 1993]. The coral samples analyzed herein span σ_θ 27.1–27.7, equivalent to a depth range of 634–2055 m, and are bathed in oxygen-depleted waters of the CCS.

In addition to existing Ba_{SW} data collected from the GEOSECS test station in 1969 [*Wolgemuth*, 1970], a new Ba_{SW} profile was obtained to compare against the coral Ba/Ca data (Figure 1). Samples were collected at Station 12 of "IrnBru" (MV1504; 39.00°N, 125.75°W). The Ba_{SW} profile is a composite of trace metal clean samples collected on 11 July 2014 (upper 100 m) and 13 July 2014 (100—1,500 m); no temporal offsets in Ba_{SW} between the two deployments are apparent. Dissolved barium concentrations were determined using an isotopic dilution method discussed in detail elsewhere [e.g., *Bates et al.*, 2017]. Briefly, 5 mL aliquots of each sample were weighed and spiked with an appropriate quantity of ^{135}Ba-^{136}Ba double spike to achieve a spike- to sample-derived Ba abundance ratio of unity. Barium was preconcentrated from the samples using a (Ba, Ca) CO_3 coprecipitation via dripwise addition of 1 M Na_2CO_3 solution and further purified from Ca using cation-exchange chromatography. Samples were analyzed using the ThermoFisher Neptune multicollector ICP-MS situated at the Woods Hole Oceanographic Institution Plasma Facility. Barium concentrations were

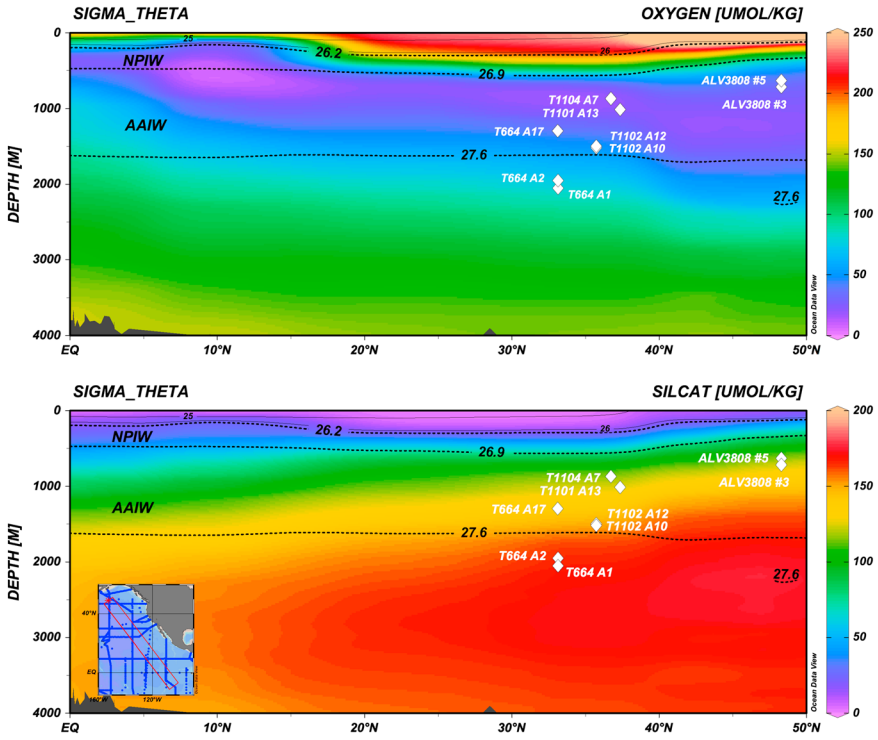

Figure 2. Coral sample locations plotted on sections (shown in inset map) of dissolved oxygen and silicate concentrations, with contours of potential density. Generated in Ocean Data View using GLODAP v1.1 gridded data [*Key et al.*, 2004; *Schlitzer*, 2016].

determined from the measured $^{138}Ba/^{135}Ba$ ion beam intensity ratio and corrected for isobaric interferences (cerium and lanthanum on *m/z* 138) and Ba contributions from reagents (average blank ≈4% of total Ba); typical precision on Ba_{SW} measurements is between 1 and 2% relative standard deviation.

2.3. Trace Element Data Collection

A disk was cut from a calcitic internode near the base of each coral and made into a thin section for trace element analysis via LA-ICP-MS. The coral samples were ablated using a Photon Machines pulsed ArF excimer 193 nm laser with HeLex dual-volume sample cell. Continuous line scans were analyzed using an 85 μm diameter circular spot, a 10 μm/second step rate, a frequency of 10 Hz, and a fluence of 4.43 J/cm^2. Ablated material was analyzed using an Agilent 7700x quadrupole ICP-MS; thorium oxides (ThO^+/Th^+) were ~0.3% for all runs. Three radial transects were drawn on each coral from the coral core to the edge. The locations of the radial transects were selected to represent as much of the coral cross section as possible and often represented varying skeletal growth rates. These transects were typically ~120° apart, except when cracks in the coral edge or thin section imperfections were avoided, in which case transects were separated by ~45–90° (T664 A17, T664 A1, T664 A2, ALV3808 #3). Three passes were completed over each radial transect with a 10 μm/s step rate, yielding two passes after the first "preablation" pass (used to remove surface contaminants) was discarded. Background intensities were obtained from gas blanks analyzed before and after sample ablation and were subtracted from coral sample ^{43}Ca and ^{138}Ba intensities, which were measured every 0.625 s. The average blank subtraction was ≪1% for both ^{43}Ca and ^{138}Ba. Coral $^{138}Ba/^{43}Ca$ count rate ratios were converted to μmol/mol using a National Institute of Standards and Technology (NIST) 612 glass standard which was analyzed at the beginning and end of each pass on the coral radial transects (n = ~10 analyses of NIST 612 per day). Raw $^{138}Ba/^{43}Ca$ count rate ratios obtained for each pass of the NIST 612 standard were reproducible within 3.4 ± 0.3% relative standard deviation (RSD) (n = 15–20 points per line), and the mean $^{138}Ba/^{43}Ca$ count rate ratios for all NIST 612 passes were highly reproducible within each day of analysis (1.6 ± 0.7% RSD; n = 10–20 passes per day). Therefore, the mean value for all NIST 612 passes (n = 10–20 per day) was applied to all coral passes analyzed on a given day, and one to two corals were analyzed per day (three to six radial transects per day).

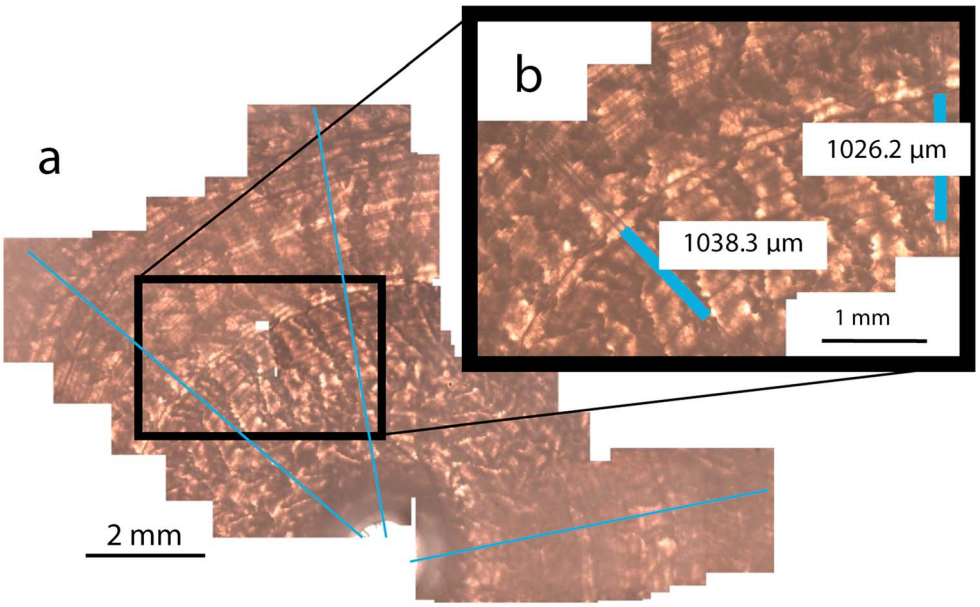

Figure 3. Growth ring alignment method. (a) Partial composite image using photomicrographs of ALV3808 #3 showing the locations of three laser ablation lines (highlighted with blue lines) and visible growth bands (alternating brown and tan rings); (b) example of the band measurement and alignment process.

2.4. Banding Analysis and Data Alignment

Bamboo corals grow radially at a rate that can vary around the coral, making each radius a different length. We used a new alignment method to compare and average LA-ICP-MS data collected from different length radii within each coral. Following LA-ICP-MS analysis of each thin section, we used a Leica Microsystems DM750P petrographic microscope with Leica Application Suite version 4.4.0 to identify and measure 5–10 visible growth bands within each coral that crossed all three laser ablation radial tracks (Figure 3). The locations of each of the growth bands on the radial laser ablation transects were used as tie points to align the trace element data from two of the radii to the length of the third, linearly interpolating between each of the tie points. Data from the second and third passes over each radius were averaged to one value for each data point after alignment (point-by-point reproducibility of replicate passes = 0.5–2.9%; Table S1 in the supporting information). This alignment method yielded satisfactory results for the eight corals with a clear banding, though sample T1102 A12 contained only a few diffuse growth bands. As such, features in this specimen could not be aligned to a resolution higher than ~200 µm. Finally, aligned raw LA-ICP-MS data from all three coral radii were resampled to a common resolution.

A 50 µm moving average was applied to each radius of Ba/Ca_{coral} data to smooth any noise resulting from ablation. After smoothing, the three replicate radii were averaged point-by-point to create a single composite record for each coral sample. Intracoral reproducibility was evaluated for each coral by calculating the point-by-point average deviation from the mean among the smoothed and aligned replicate radii.

All samples exhibited anomalously high Ba/Ca_{coral} in the inner 100–800 µm of calcite near the center of the coral (oldest material precipitated), likely reflecting the higher organic matter content of juvenile skeleton (Figure S2) [*Noe and Dullo*, 2006; *LaVigne et al.*, 2011; *Sinclair et al.*, 2011]. In some of the samples, this area appeared darker than the rest of the coral under photomicrograph. The size of the juvenile growth area varied from sample to sample; therefore, regions of elevated Ba/Ca associated with the juvenile growth area were identified separately for each coral and removed from subsequent analysis.

3. Results and Discussion

3.1. Accuracy of Ba/Ca_{coral} LA-ICP-MS Measurements

Laser ablation ICP-MS offers a rapid means of obtaining high resolution trace elemental data from samples in situ. Although this technique has long been used to analyze elemental ratios in carbonates for

Table 2. Bamboo Coral Ba/Ca, Reconstructed Ba_{SW}, and Internal Reproducibility

Sample	Solution Phase Ba/Ca (μmol/mol) Outer 1 mm [*LaVigne et al.*, 2011]	LA-ICP-MS Ba/Ca (μmol/mol) Outer 1 mm This Study ±1 SD	Reconstructed Ba_{SW} (nmol/kg) Outer 1 mm This Study ±1 SD	Internal Reproducibility of Raw LA-ICP-MS Data ±1 SD (%, n = 3)	Internal Reproducibility With 9-Point (50 μm) Smoothing ±1 SD (%, n = 3)	Internal Reproducibility After Smoothing and Peak Removal (%, n = 3)
ALV3808 #5	-	9.75 ± 0.26	73 ± 3	1.5 ± 0.8	1.1 ± 0.7	-
ALV3808 #3	-	10.30 ± 0.22	80 ± 3	0.9 ± 0.5	0.8 ± 0.5	-
T1104 A7	14.48 ± 0.47	13.67 ± 0.71	120 ± 18	8.8 ± 5.7	7.8 ± 5.3	6.7 ± 4.0
T1101 A13	12.21 ± 0.47	13.47 ± 0.79	117 ± 13	4.2 ± 3.4	3.5 ± 2.9	3.2 ± 2.6
T664 A17	13.15 ± 0.47	12.98 ± 0.17	111 ± 4	2.6 ± 1.8	2.1 ± 1.4	1.9 ± 1.1
T1102 A12	15.46 ± 0.47	17.02 ± 1.71	162 ± 14	5.0 ± 4.5	4.0 ± 4.0	4.1 ± 4.1
T1102 A10	15.88 ± 0.47	16.41 ± 0.61	155 ± 11	4.4 ± 3.6	3.7 ± 3.1	3.2 ± 2.4
T664 A2	15.35 ± 0.47	16.19 ± 0.15	152 ± 4	2.1 ± 1.2	1.6 ± 1.0	1.1 ± 0.7
T664 A1	14.71 ± 0.47	15.99 ± 0.10	149 ± 3	1.8 ± 1.3	1.0 ± 1.0	0.8 ± 0.5

paleoceanographic reconstructions, the development of appropriate matrix-matched standards for quantifying trace elements in carbonates remains challenging [e.g., *Sinclair et al.*, 1998]. Glass NIST standards (e.g., NIST 610, 612, and 614) are commonly used for single-point nonmatrix matched standardization of trace elemental signals in carbonates. The accuracy of this technique, however, is limited by the potential for matrix-induced elemental fractionation during sample ablation, transport, and/or within the plasma [*Sinclair et al.*, 1998; *Fallon et al.*, 1999; *Sylvester*, 2008]. Some laboratories have developed in-house or interlab external standards from pressed-carbonate powder pellets (e.g., MACS-1 and MACS-3: U.S. Geological Survey) [*Sinclair et al.*, 1998; *Fallon et al.*, 1999], though the ablation characteristics of pressed-powder pellets may differ from solid biogenic carbonates. While commercially available matrix-matched standards continue to be developed, we evaluated the accuracy of our LA-ICP-MS data for Ba/Ca in bamboo corals via comparison with Ba/Ca data obtained for the same samples using solution ICP-MS [*LaVigne et al.*, 2011].

We tested this accuracy by comparing LA-ICP-MS data generated using a single-point glass NIST SRM standard (612) against solution phase high-resolution-ICP-MS data collected on the same set of samples using NIST-traceable matrix-matched standard curves [*LaVigne et al.*, 2011]. For five of the seven samples, we found that the average Ba/Ca_{coral} value for the outer ~1 mm of LA-ICP-MS data determined in this study overlaps within the uncertainty of published solution phase ICP-MS measurements in powders milled from the outer 1 mm of the same specimens (Table 2 and Figure 4). For the two samples that did not overlap within the uncertainty of the measurements, T664A1 and T664A2, the envelopes of uncertainty differed by $<5\%$ (Table 2 and Figure 4). This minor difference is possibly due to the comparison of samples collected from different sections cut from the calcitic internodes. The general consistency between the two methods demonstrates the accuracy of using the NIST 612 glass as a single-point standard for quantifying Ba/Ca_{coral} via LA-ICP-MS. This suggests that differential plasma matrix effects between the NIST 612 silicate glass standard and the biogenic high magnesium calcite samples are either minimal or affect Ba and Ca similarly. This comparison allows for the application of Ba/Ca_{SW} calibrations calculated using solution-phase ICP-MS measurements to LA-ICP-MS Ba/Ca_{coral} data.

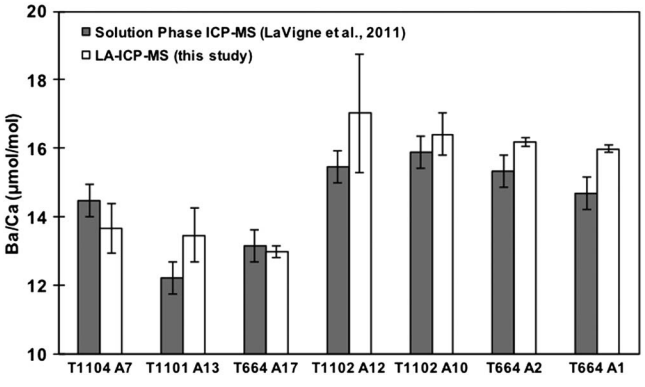

Figure 4. Comparison of Ba/Ca_{coral} measurements collected on the outer 1 mm of the same set of coral samples via LA-ICP-MS using single-point glass NIST SRM standard (612; this study; white) and solution phase high-resolution-ICP-MS data using NIST-traceable matrix-matched standard curves [*LaVigne et al.*, 2011] (grey). Error bars represent measurement uncertainty (Table 2).

3.2. Resolution of LA-ICP-MS Ba/Ca$_{coral}$ Data

In order to identify the smoothing window required to remove laser ablation noise and fine-scale sample heterogeneity, we optimized the intracoral reproducibility across all corals investigated. After testing 10 different smoothing windows of varying widths (10–200 μm), we found that applying a 50 μm (9-point) moving average yielded the greatest degree of Ba/Ca$_{coral}$ reproducibility without significantly changing the data from the unsmoothed version (paired *t* test, $p > 0.05$ for smoothing windows 10–50 μm). The 50 μm smoothing window we found to be optimal for our data obtained with an 85 μm spot is comparable to the 40 μm window that *Sinclair et al*. [2011] found to be optimal for Ba/Ca data from an Atlantic bamboo coral specimen using a 60 μm spot size. Mean point-by-point Ba/Ca reproducibility for all nine corals improved from 3.5% to 2.8% after the 9-point (50 μm) moving average smoothing window was applied (Table 2). We estimate that the 50 μm smoothing window (85 μm initial spot size plus the 50 μm window yields an approximately 135 μm spatial resolution) results in ~1.5–2 year temporal resolution based on the average growth rates estimated for these corals (Table 1). Increased reproducibility after application of the 50 μm moving average suggests that any variability that occurs on spatial scales <135 μm is related to laser noise, and/or fine-scale localized Ba/Ca$_{coral}$ heterogeniety. All data discussed from this point forward were smoothed via this process.

3.3. Temporal Variations in Skeletal Ba/Ca: Artifact or Ambient Environmental Variability?

The records derived from these corals reveal temporal Ba/Ca$_{coral}$ variability that differs with depth, location, and time (Figures 5 and 6). While Gulf of Alaska (634–720 m) and southern California (San Juan Seamount, 1295 m and 1954–2055 m) samples imply relatively stable Ba/Ca throughout the lifetime of the corals (±2–3%; 1 RSD), the central California seamount corals collected from near or within the severely to intermediately hypoxic waters of the OMZ reveal a greater degree of temporal Ba/Ca variability (5–10%; 1 RSD; Figures 5 and 6). Even though several of the most variable corals lack precise chronologies, based on the spatial scales of the Ba/Ca$_{coral}$ variations (~100 μm to ~1 mm) and average coral radial extension rates (~70–160 μm/yr in well-dated specimens [*Roark et al*., 2005; *Hill et al*., 2014]), we estimate that the timescale of the largest Ba/Ca variations evident in Figure 5 is interannual to decadal. This is consistent with the timescale of variability observed in other Ba/Ca$_{coral}$ records [*Sinclair et al*., 2011; *LaVigne et al*., 2011; *Strzepek et al*., 2014]. Next we explore whether such temporal variations are likely derived from either analytical or biological artifacts that impact internal reproducibility, or if they might reflect true variability in ambient Ba$_{SW}$.

3.3.1. Potential Artifacts Affecting Internal Reproducibility

To explore if the observed temporal Ba/Ca variations relate to an analytical or biological artifact, we first quantified intracoral reproducibility by calculating the percent average deviation from the mean for each individual point in the aligned and smoothed radial transects ($n = 3$ replicate radii), and the mean percent deviation for the entire coral is reported in Table 2. The smoothed and aligned replicate Ba/Ca radii were highly reproducible (1–4%) for eight of the nine northeast Pacific *Isidella*, *Lepidisis*, and *Keratoisis* corals analyzed (Table 2; slightly lower reproducibility (6.7%) for one coral, T1104 A7, is discussed below). This is consistent with the level of reproducibility reported by *Sinclair et al*. [2011] whereby a similar analysis was performed for Ba/Ca$_{coral}$ data from an Atlantic *Keratoisis* specimen (4%). *Strzepek et al*. [2014] also reported similar reproducibility of 1.4% based on mean Ba/Ca values from repeat LA-ICP-MS transects in a *Lepidisis sp*. coral collected southeast of Australia at 1160 m depth. However, difficulties associated with determining accurate bamboo coral taxonomy suggest that it is necessary to validate any new geochemical proxies in multiple taxa collected from various environments before records can be confidently interpreted.

The intracoral Ba/Ca reproducibility demonstrated by the eight corals spanning three taxa, combined with evidence from the *Keratoisis* coral published by *Sinclair et al*. [2011], suggests that Ba/Ca$_{coral}$ records are internally reproducible across multiple taxa and geographic locations. However, some samples in our study showed lower reproducibility among select peaks in the Ba/Ca radial transects that emphasize the importance of replication and multielement screening of LA-ICP-MS data (e.g., T1104 A07, T1101 A13, and T1102 A12; Figure 5). The lowest reproducibility for peaks in these samples was ~20%. The reduced reproducibility of peaks in these samples is likely a result of differences in the degree of signal smoothing resulting from varying growth rates between replicate radii. Additionally, some of these peaks may reflect noncarbonate phases containing Ba, such as organic seams (discussed below). Furthermore, we note that sample T664 A2 showed Ba/Ca$_{coral}$ values in the outer 1.3 mm of one radius (line 2) that were ~7% higher than the two

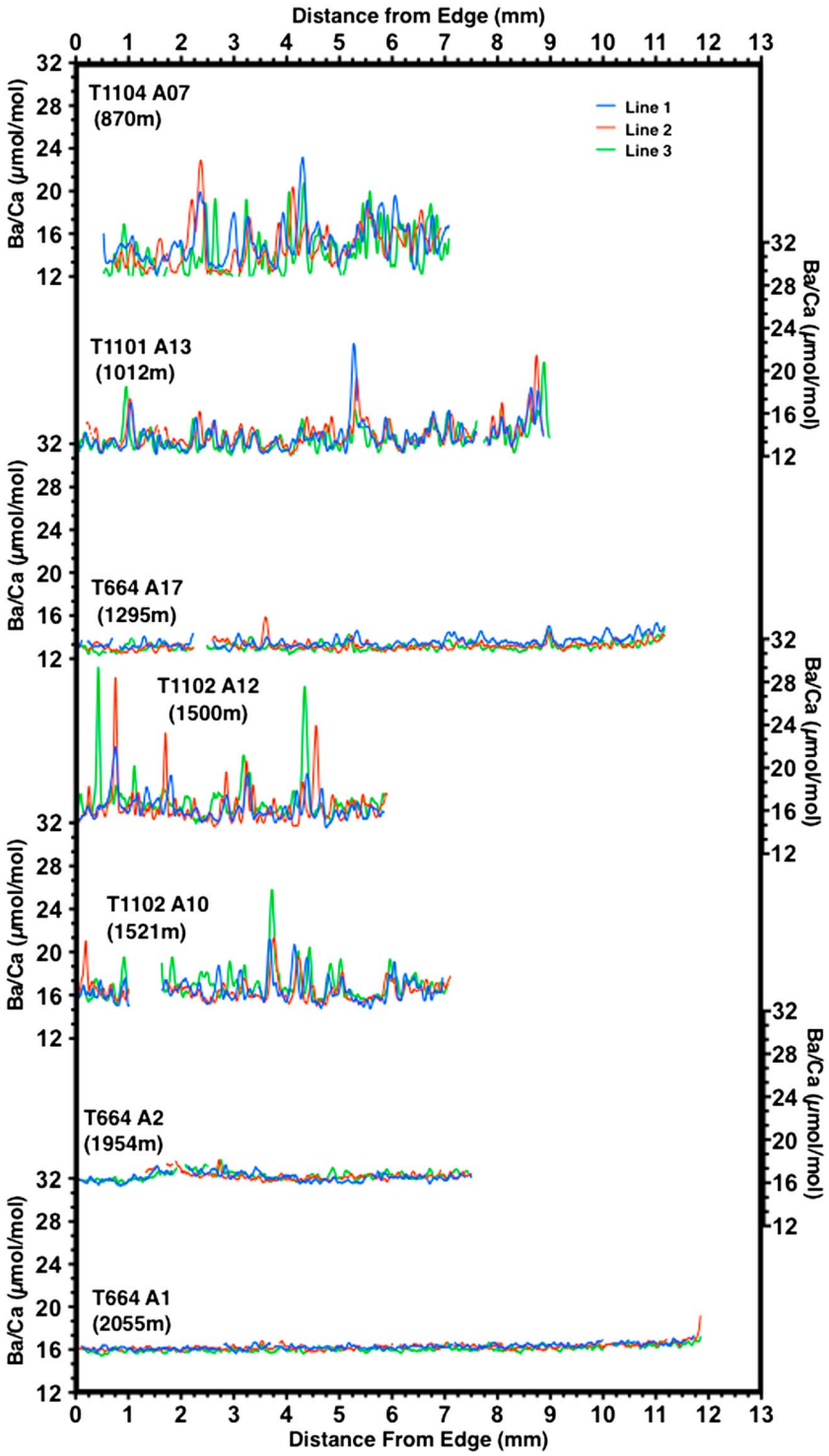

Figure 5. Ba/Ca LA-ICP-MS measurements across replicate radial transects (n = 3 transect lines; blue, red, and green) for each of seven bamboo corals from the California margin. Replicate passes on individual radial transect have been averaged to a single record for each line and smoothed with a 9-point moving average. Internal reproducibility calculated based on agreement among three replicate radii for each coral and reported in Table 2.

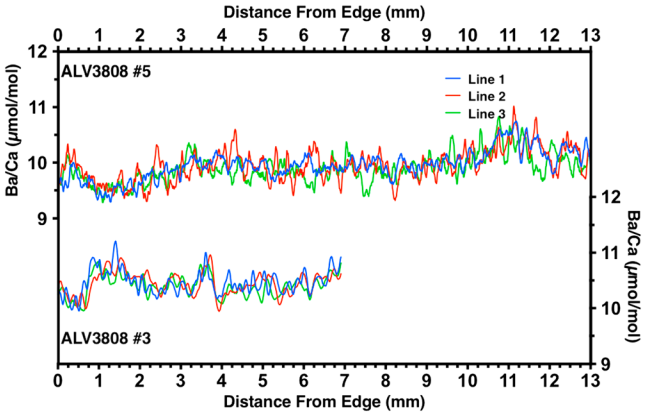

Figure 6. Ba/Ca LA-ICP-MS measurements across replicate radial transects (n = 3 transect lines; blue, red, and green) for each of two bamboo corals from the Gulf of Alaska. Replicate passes on individual radial transect have been averaged to a single record for each line and smoothed with a 9-point moving average. Internal reproducibility calculated based on agreement among three replicate radii for each coral and reported in Table 2.

replicate radii (lines 1 and 3, which agreed within 1%; Figure 5). The elevated Ba/Ca values were present in the outer 1.3 mm of all three passes along line 2, eliminating the possibility that analytical uncertainty yielded the anomaly. Inspection of the sample in thin section did not reveal any visual differences in the coral calcite between line 2 and lines 1 and 3. A more thorough spatial Ba/Ca_{coral} analysis around the edge of this coral would be required to determine the cause of this small anomaly on line 2. Although internal reproducibility for the entire T664 A2 record was overall good (1.6%), in order to avoid interpreting this anomalous area, the data from the last 1.3 mm of line 2 were excluded from further analyses (resulting in 1.1% intracoral reproducibility; Table 2 and Figure S2). Sample T1104 A7 was the least internally reproducible sample analyzed (6.7%); however, T1104 A7 did not show a consistently offset portion of a radius similar to that found in T664 A2. This specimen was, however, the sample that exhibited the greatest degree of variability (±10%; 1 RSD) with large Ba/Ca peaks evident throughout the record. Based on visual inspection of the replicate radial Ba/Ca transects, we suspect that our growth band alignment method did not perfectly align these large peaks in this record, and that a more precise manual alignment of Ba/Ca peaks would likely result in greater reproducibility for this coral (and may also account for slight offsets of large peaks in other corals, e.g., T1102 A12). These two corals (T664 A2 and T1104 A7) demonstrate the importance of collecting replicate radial transects, visually inspecting thin sections and checking data alignment in order to evaluate intracoral reproducibility for every specimen analyzed prior to interpreting Ba/Ca records.

The intracoral Ba/Ca agreement evident in these corals demonstrates that time-resolved Ba/Ca_{coral} signals are generally incorporated reproducibly around the entire circumference of the coral. We note, however, that the scale upon which this agreement is evident varies among the records. For example, there are fine scale ($<$0.2–0.5 mm) Ba/Ca_{coral} variations on the order of ~0.5–1.0 μmol/mol in some of the least variable corals (e.g., ALV3808#5, T664 A2, and T664 A17) that were not evident in all three replicate transects. Thus, the temporal resolution upon which the Ba/Ca_{coral} records can be interpreted would depend on both the degree of reproducibility among replicate transects and the growth rate of each coral. Averaging three aligned transects into a single composite record for each coral would likely minimize and avoid interpretation of nonreproducible compositional heterogeneities in the coral skeleton. Overall, these results support the suggestion that the entire coral skeleton records interannual to decadal scale variability [*Sinclair et al.*, 2011], likely in response to changes in environmental conditions rather than internal biological "vital effects," which have been implicated in non-reproducible behavior of other trace elemental ratios in bamboo coral skeletons. The radial Ba/Ca_{coral} signals we observe are not driven by localized vital effects specific to the calcification sites on different growth axes within the same coral. However, possible biological factors affecting the incorporation of barium around the entire coral cannot be ruled out with this data set. It is possible that factors such as skeletal extension rate, for example, could be consistent among all growth axes. Though, given that mean Ba/Ca_{coral} values for replicate radii with different radial extension rates agreed within each coral in our study, we argue that changes in skeletal growth rate with time are not likely to have caused the observed temporal reproducibility.

Although it is unlikely that growth rate was a driver of Ba/Ca_{coral} variability in our corals, *Sinclair et al.* [2011] also point out that nonenvironmental factors such as intermittant bands or seams of organic-rich skeleton or detritus could also result in intracoral Ba/Ca reproducibility. Thus, we investigated whether these sources of

Ba could be influencing the Ba/Ca_{coral} signals in our corals by screening our records for regions where Ba/Ca_{coral} was correlated with Mg/Ca and Pb/Ca as well as visually inspecting calcite thin sections. Mg/Ca has been used to identify and remove regions of trace elemental proxy data influenced by organic matter inclusions in centers of calcification in scleractinian deep sea corals; we also observed elevated Mg/Ca in juvenile bamboo coral skeleton, which likely represents a different phase of skeletal growth [e.g., *Cohen et al.*, 2006; *Gagnon et al.*, 2007; *Thresher et al.*, 2010; *Anagnostou et al.*, 2011; *Sinclair et al.*, 2011]. Given that the incorporation of detritus or Pb adsorption to skeletal surfaces exposed to seawater during a coral's lifetime has been suggested to contribute to elevated Pb/Ca ratios in bamboo coral skeletons, we screened our LA-ICP-MS data for Pb/Ca as well as Mg/Ca anomalies [*Sinclair et al.*, 2011]. In our corals, large Mg/Ca and Pb/Ca anomalies were often found in regions where the calcite appears visually distinct in photomicrographs and are thus used as indicators of noncarbonate phases (Figure S1). We identified possible regions of noncarbonate bound barium in individual radial transects in the California margin coral data sets as regions where either the smoothed Pb/Ca or Mg/Ca data were more than ±2 standard deviations from the radial transect mean. Inspection of photomicrographs of the calcite thin sections revealed that distinct dark or light skeletal rings often occurred close to these Mg/Ca or Pb/Ca anomalies. Regions of Ba/Ca records where corresponding Mg/Ca or Pb/Ca fell outside of the ±2 SD envelope as well as values associated with these features that were immediately preceeding or following the peaks were removed from the data set and were not used in subsequent analyses. For most lines, this process removed $<$10% of the record. This process was not completed for the Gulf of Alaska coral data because we did not collect Pb/Ca data nor have appropriate thin sections for visual inspection. An example of anomalous features identified in sample T664 A17 is shown in Figure S1 and a side-by side comparison of filtered and unfiltered Ba/Ca data for all coral plotted in Figure 5 is shown in Figure S2. The removal of these anomalous regions did not change (or only slightly improved) intracoral Ba/Ca_{coral} reproducibility (Table 2). The features support the hypothesis that trace elemental proxy data may be influenced by organic seams or cessations of growth which allowed detritus from surrounding seawater to be skeletally incorporated, and that these features may be identified by screening ancillary trace elemental data [*Sinclair et al.*, 2011]. These observations encourage careful replication and further development of this multielement screening technique to identify possible noncarbonate bound phases of trace elements in bamboo coral LA-ICP-MS data.

3.3.2. Ambient Environment Variability

Our analysis appears to rule out either analytical or biological artifacts as the cause of radial Ba/Ca_{coral} variability, suggesting instead that the variations reflect changes in conditions ambient to the corals. We contend that such variations most likely reflect changes in ambient Ba_{SW} rather than a changing partition coefficient (D), since changes in D resulting from environmental perturbations (e.g., $[O_2]$, temperature, and salinity) might also be expected to render changes in the partitioning of other elements and thus lead to correlated metal: calcium variability along the coral transects [e.g., *Gagnon et al.*, 2007]. Since it appears that these variations are largely uncorrelated with Ba/Ca_{coral} after performing the screening technique described above ($r^2 < 0.2$ for Ba/Ca versus Pb/Ca, Mg/Ca, B/Ca, Sr/Ca, and Li/Ca), we are left with the explanation that the changes in Ba/Ca_{coral} reflect interannual-to-decadal variability in ambient Ba_{SW}. Though we currently lack the chronologies required to align the records in time, the similar magnitudes and variance in Ba/Ca_{coral} from specimens that were either colocated (e.g., T1102 A10 and T1102 A12) or situated within 100 m of another individual (T664 A2 and T664 A1 (collected dead); ALV3808 #3 and ALV3808 #5) is encouraging as it supports our contention that Ba_{SW} is variable, particularly in low-oxygen environments.

In order to place the observed degree of Ba/Ca_{coral} variability in an oceanographic perspective, we calculated the mean value and magnitude of variation in reconstructed Ba_{SW} for each coral using the calibration published in *LaVigne et al*. [2011] and compared against measured profiles of Ba_{SW} from the northeast Pacific (Figure 7). Mean "modern" values of Ba_{SW} were calculated from the outer (youngest) ~1 mm, or ~6–14 years, of each coral record (excluding the juvenile growth phase and possible noncarbonate phases as described in sections 2.4 and 3.3.1). The standard deviation of the entire coral record (not just the outer 1 mm) is interpreted as the magnitude of long-term variability. Analysis of the data obtained via these calculations yields two main results. First, as observed in the solution phase ICP-MS-based calibration by *LaVigne et al*. [2011], the calculations suggest that there are substantial mismatches in reconstructed Ba_{SW} of ~25–40 nmol/kg when comparing coral-derived Ba_{SW} against in situ Ba_{SW} from the GEOSECS test station at ~30°N (Figure 1). However, when comparing the reconstructed Ba_{SW} against a new Ba_{SW} profile collected along the

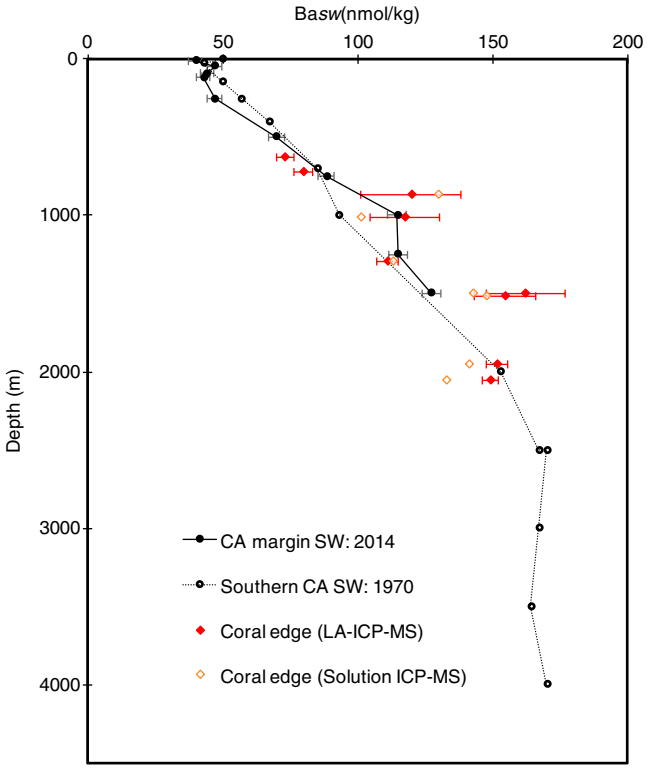

Figure 7. Ba_{SW} values reconstructed from bamboo coral Ba/Ca (diamonds) using the *LaVigne et al.* [2011] calibration equation for nine coral Ba/Ca records compared against in situ Ba_{SW} profiles from the east Pacific margin: GEOSECS test station: 28.483°N, 121.633°W (open black circles) [*Wolgemuth*, 1970] and northern California margin (filled circles plotted with ±2 SD; MV1405 St. 12; 39.00°N, 125.75°W). Ba_{SW} calculated from Ba/Ca_{coral} values measured in the outer 1 mm of skeleton via LA-ICP-MS (filled red diamonds; Table 2) and solution phase ICP-MS (open red diamonds) [*LaVigne et al.*, 2011] are plotted with ±1 SD of LA-ICP-MS measurements along the entire coral record to represent temporal variability (shown as red x-error bar).

California margin in 2014 (~40°N), we find that the mismatch decreases to ~5–35 nmol/kg (Figure 7). A large offset was observed in specimen T1104 A7, which was collected within Monterey Canyon. As such, the reconstructed Ba_{SW} from this sample may be reflecting sources of barium specific to the canyon environment (e.g., continental, sedimentary, seeps, organic, or detrital Ba sources; Figure 7). Interestingly, the Ba_{SW} values calculated from the Davidson Seamount samples are also offset from the dissolved barium transect, similar to the Ba/Ca_{coral} variability with depth observed in this region by *LaVigne et al.* [2011] and in southern Tasmania by *Thresher et al.* [2016]. Thus, bamboo coral Ba/Ca records may have the potential to provide regional- or even local-scale records of seawater chemistry, offering a unique window into the spatial variability of barium dynamics.

Our data also reveal that the variation in reconstructed Ba_{SW} appears greatest within the severely to intermediately hypoxic waters of the OMZ (corals between 870 and 1521 m), consistent with measurements of highly variable barium dynamics in oxygen minima at this depth range (Figure 2) [*Dymond and Collier*, 1996; *Dehairs et al.*, 1980, 1991, 1992, 2008]. Marine barium dynamics are generally controlled by processes associated with the near-surface cycling of nutrients, carbon, and barite [e.g., *Dehairs et al.*, 1980; *Bishop*, 1988] that are communicated to the ocean interior [e.g., *Horner et al.*, 2015]. For example, changes in wind-driven coastal upwelling in this region have a significant effect on productivity in surface waters [e.g., *Snyder et al.*, 2003; *Garcia-Reyes and Largier*, 2010], which has been shown to drive high rates of intermediate ocean barite production in this region [*Dymond et al.*, 1992]. However, given that these same coral specimens record negligible changes in the export of organic matter from the surface [*Hill et al.*, 2014], the most likely source of changes in Ba_{SW} would be processes occurring at depth rather than any direct connection to local surface productivity and export. As a rough estimate, if barite dynamics were solely responsible for the Ba_{SW} variations recorded by these corals, in order to effect a ~ 70 nmol/kg increase in dissolved barium between 1000–1500 m depth within ~10 years, the flux of particulate barium to this depth would need to increase by ~3.5 mmol Ba m^2 yr^{-1}, which is only about 3 times higher than the highest particulate barium flux measurements from ~1000 to 2000 m CCS sediment traps (~1.2 mmol Ba m^2 yr^{-1}) [*Dymond et al.*, 1992]. While this scale of change in biogenic particle flux would be conceivable for the coastal CCS upwelling zone, it is also possible that multiple mechanisms work concurrently to influence Ba_{SW} on interannual-decadal timescales. Moreover, Ba/Ca_{coral} variability evident from corals of different latitudes within the OMZ hints at spatially variable Ba dynamics within intermediate waters along the California margin (Figure S3). Further development of the

Ba/Ca_{coral} proxy, together with accurately dated Ba/Ca records from additional coral specimens, thus have the potential to elucidate both the temporal and spatial patterns of intermediate- and deep-water dynamics.

4. Conclusions

The results of this study add to the growing body of evidence supporting Ba/Ca_{coral} as a proxy for ambient and past Ba_{SW} which now includes (1) a strong linear relationship (calibration) between Ba/Ca_{coral} and ambient Ba_{SW} [*LaVigne et al.*, 2011; *Thresher et al.*, 2016]; (2) a barium partition coefficient (D) for bamboo corals with remarkable agreement to that of aragonitic surface and deep-sea corals ($D \sim 1$), suggesting that Ba is incorporated via cationic substitution [*Anagnostou et al.*, 2011; *LaVigne et al.*, 2011, 2016]; (3) evidence for internally reproducible Ba/Ca_{coral} time series in multiple bamboo coral taxa and geographic regions [*Sinclair et al.*, 2011; *Strzepek et al.*, 2014; this study]; and (4) a lack of covariation between Ba/Ca and other trace elements after regions where noncarbonate phases are identified and removed from the data set (e.g., organic matter or detritus).

Furthermore, the data presented here demonstrate the accuracy of using LA-ICP-MS to quantify Ba/Ca_{coral} as well as a high degree of reproducibility in decade-to-century-scale Ba/Ca_{coral} variability preserved in eight bamboo corals collected along an eastern Pacific depth transect. This reproducibility encourages further validation of the use of Ba/Ca_{coral} to reconstruct past changes in dissolved barium concentrations, which has been linked to several biogeochemical processes such as the cycling and export of nutrients, organic carbon, and barite in surface and intermediate oceans. Coral records from ~900 to 1500 m depths imply subdecadal increases in Ba/Ca_{SW} of ~10–70 nmol/kg Ba_{SW} at depths where rapid barite cycling has been shown to occur on daily weekly timescales in other regions [e.g., *Bishop and Wood*, 2008]. The interannual scale Ba_{SW} peaks recorded by corals located near the most oxygen-depleted water in the CCS OMZ may reflect changes in intermediate water circulation or periods of decreased barite formation (and/or increased dissolution) via reduced bacterial C_{org} respiration or altered barite saturation state. Continued validation of the Ba/Ca_{coral} proxy by investigating intercoral reproducibility among colocated corals, phases of barium incorporation, and other tracers of Ba in seawater (e.g., barium isotopes) along with continued research on barium cycling in the modern ocean has the potential to elucidate the mechanisms linking intermediate water barium cycling to carbon cycling, ocean circulation, and climate.

Acknowledgments

Data from this study can be found in the supporting information (Data Set S1) and on the NOAA paleoclimate database (https://www.ncdc.noaa.gov/paleo/study/22475) with no restrictions on access. This research was funded by NSF grant OCE-1420984 to M. LaVigne, a Bowdoin College Gibbons Summer Research Fellowship to G. Serrato Marks, and a UC Davis President's Undergraduate Fellowship to W. Sauthoff. An American Geophysical Union Travel Grant and support from the MIT-WHOI Joint Program provided funds for G. Serrato Marks to attend the AGU 2014 and 2015 Fall Meetings to present this work and receive valuable feedback. The authors thank J. Fehrenbacher, H. Spero, and A. Russell at UC Davis for assistance with laser ablation analyses, M. Frenkel and H. Miller for assistance with data processing, and J. Ptacek and B. Geyman for valuable discussions and CA margin dissolved Ba analyses. Comments from an anonymous reviewer greatly improved the quality of this manuscript. Special thanks to the crew and scientific parties of GoASEx R/V *Atlantis* cruise for Gulf of Alaska corals collected using DSRV *Alvin* (NOAA/OE NA16RP2637 to T. Guilderson) and to Monterey Bay Aquarium Research Institute (MBARI) R/V *Western Flyer* Seamounts Expeditions in 2004 and 2007 for California margin corals collected by ROV *Tiburon* (grant to MBARI from the David and Lucile Packard Foundation). We thank Claire Till for providing seawater samples from MV1405 IrnBru. A portion of this work was performed at the U.S. DOE Lawrence Livermore National Laboratory under contract DE-AC52-07NA27344. G. Serrato Marks completed this work as an undergraduate research student in M. LaVigne's laboratory at Bowdoin College.

References

Adkins, J., H. Cheng, E. Boyle, and E. Druffel (1998), Deep-sea coral evidence for rapid change in ventilation of the deep North Atlantic 15,400 years ago, *Science*, *280*, 725–728, doi:10.1126/science.280.5364.725.

Ainley, D., and K. Hyrenbach (2010), Top-down and bottom-up factors affecting seabird population trends in the California current system (1985–2006), *Prog. Oceanogr.*, *84*, 242–254, doi:10.1016/j.pocean.2009.10.001.

Anagnostou, E., R. Sherrell, A. C. Gagnon, M. LaVigne, M. P. Field, and W. F. McDonough (2011), Seawater nutrient and carbonate ion concentrations recorded as P/Ca, Ba/Ca, and U/Ca in the deep-sea coral Desmophyllum dianthus, *Geochim. Cosmochim. Acta*, *75*, 2529–2543, doi:10.1016/j.gca.2011.02.019.

Andrews, A. H., G. M. Cailliet, L. A. Kerr, K. Coale, C. Lundstrom, and A. P. DeVogelaere (2005), Investigations of age and growth for three deep-sea corals from the Davidson Seamount off central California, *Cold-Water Corals Ecosystems*, *1021–1038*, doi:10.1007/3-540-27673-4_51.

Bates, S. L., K. R. Hendry, H. V. Pryer, C. W. Kinsley, K. M. Pyle, E. M. S. Woodward, and T. J. Horner (2017), Barium isotopes reveal role of ocean circulation on barium cycling in the Atlantic, *Geochim. Cosmochim. Acta*, *204*, 286–299, doi:10.1016/j.gca.2017.01.043.

Bishop, J. K. B. (1988), The barite–opal–organic carbon association in oceanic particulate matter, *Nature*, *332*, 341–343, doi:10.1038/332341a0.

Bishop, J., and T. J. Wood (2008), Particulate matter chemistry and dynamics in the twilight zone at VERTIGO ALOHA and K2 sites, *Deep Sea Res., Part I*, *55*, 1684–1706, doi:10.1016/j.dsr.2008.07.012.

Cohen, A., G. Gaetani, T. Lundälv, B. Corliss, and R. George (2006), Compositional variability in a cold-water scleractinian, Lophelia pertusa: New insights into "vital effects", *Geochem. Geophys. Geosyst.*, *7*, Q12004, doi:10.1029/2006GC001354.

Dehairs, F., R. Chesselet, and J. Jedwab (1980), Discrete suspended particles of barite and the barium cycle in the open ocean, *Earth Planet. Sci. Lett.*, *49*, 528–550, doi:10.1016/0012-821X(80)90094-1.

Dehairs, F., N. Stroobants, and L. Goeyens (1991), Suspended barite as a tracer of biological activity in the Southern Ocean, *Mar. Chem.*, *35*, 399–410, doi:10.1016/s0304-4203(09)90032-9.

Dehairs, F., W. Baeyens, and L. Goeyens (1992), Accumulation of barite at mesopelagic depths and export production in the Southern Ocean, *Science*, *258*, 1332–1335, doi:10.1126/science.258.5086.1332.

Dehairs, F., et al. (2008), Barium in twilight zone suspended matter as a potential proxy for particulate organic carbon remineralization: Results for the North Pacific, *Deep Sea Res., II*, *55*(14–15), 1673–1683, doi:10.1016/j.dsr2.2008.04.020.

Deutsch, C., H. Brix, T. Ito, H. Frenzel, and L. Thompson (2011), Climate-forced variability of ocean hypoxia, *Science*, *333*(6040), 336–339, doi:10.1126/science.1202422.

Dymond, J., and R. Collier (1996), Particulate barium fluxes and their relationships to biological productivity, *Deep Sea Res., Part II*, *43*(4–6), 1283–1308, doi:10.1016/0967-0645(96)00011-2.

Dymond, J., E. Suess, and M. Lyle (1992), Barium in deep-sea sediment: A geochemical proxy for paleoproductivity, *Paleoceanography*, *7*(2), 163–181, doi:10.1029/92PA00181.

Esser, B. K., and A. M. Volpe (2002), At-sea high-resolution chemical mapping: Extreme barium depletion in North Pacific surface water, *Mar. Chem.*, *79*, 67–79, doi:10.1016/S0304-4203(02)00037-3.

Fallon, S., M. McCulloch, R. van Woesikb, and D. Sinclair (1999), corals at their latitudinal limits: Laser ablation trace element systematics in Porites from Shirigai Bay, Japan, *Earth Planet. Sci. Lett.*, *172*(3–4), 221–238, doi:10.1016/S0012-821X(99)00200-9.

Farmer, J. R., B. Hönisch, L. F. Robinson, and T. M. Hill (2015a), Effects of seawater-pH and biomineralization on the boron isotopic composition of deep-sea bamboo corals, *Geochim. Cosmochim. Acta*, *155*, 86–106, doi:10.1016/j.gca.2015.01.018.

Farmer, J. R., L. F. Robinson, and B. Hönisch (2015b), Growth rate determinations from radiocarbon in bamboo corals (genus *Keratoisis*), *Deep Sea Res., Part I*, *105*, 26–40, doi:10.1016/j.dsr.2015.08.004.

France, S. C. (2007), Genetic analysis of bamboo corals (Cnidaria: Octocorallia: Isididae): Does lack of colony branching distinguish Lepidisis from Keratoisis?, *Bull. Mar. Sci.*, *81*, 323–333.

Frenkel, M. M., M. LaVigne, H. R. Miller, T. M. Hill, A. McNichol, and M. Lardie Gaylord (2017), Quantifying bamboo coral growth rate nonlinearity with the radiocarbon bomb spike: A new model for paleoceanographic chronology development, *Deep Sea Res., Part I*, *125*, 26–39, doi:10.1016/j.dsr.2017.04.006.

Gagnon, A. C., J. F. Adkins, D. P. Fernandez, and L. F. Robinson (2007), Sr/Ca and mg/Ca vital effects correlated with skeletal architecture in a scleractinian deep-sea coral and the role of Rayleigh fractionation, *Earth Planet. Sci. Lett.*, *261*, 280–295, doi:10.1016/j.epsl.2007.07.013.

Garcia-Reyes, M., and J. Largier (2010), Observations of increased wind-driven coastal upwelling off central California, *J. Geophys. Res.*, *115*, C04011, doi:10.1029/2009JC005576.

Heikoop, J. M., D. D. Hickmott, M. J. Risk, and C. K. Shearer (2002), Potential climate signals from the deep-sea gorgonian coral Primnoa resedaeformis, *Hydrobiologia*, *471*, 117–124, doi:10.1023/a:1016505421115.

Hill, T. M., H. J. Spero, T. P. Guilderson, M. LaVigne, D. A. Clague, S. Macalello, and N. Jang (2011), Temperature and vital effect controls on bamboo coral (Isididae) isotope geochemistry: A test of the "lines method", *Geochem. Geophys. Geosyst.*, *12*, Q04008, doi:10.1029/2010GC003443.

Hill, T. M., M. LaVigne, H. J. Spero, T. Guilderson, B. Gaylord, and D. Clague (2012), Variations in seawater Sr/Ca recorded in deep-sea bamboo corals, *Paleoceanography*, *27*, PA3202, doi:10.1029/2011PA002260.

Hill, T. M., C. R. Myrvold, H. Spero, and T. Guilderson (2014), Evidence for benthic-pelagic food web coupling and carbon export from California margin bamboo coral archives, *Biogeosciences*, *11*, 3845–3854, doi:10.5194/bgd-11-2595-2014.

Horner, T. J., C. W. Kinsley, and S. G. Nielsen (2015), Barium-isotopic fractionation in seawater mediated by barite cycling and ocean circulation, *Earth Planet. Sci. Lett.*, *430*, 511–522, doi:10.1016/j.epsl.2015.07.0270012-821X.

Howell, E. A., S. J. Bograd, C. Morishige, and M. P. Seki (2012), On North Pacific circulation and associated marine debris concentration, *Mar. Pollut. Bull.*, *65*, 16–22, doi:10.1016/j.marpolbul.2011.04.034.

Karstensen, J., L. Stramma, and M. Visbeck (2008), Oxygen minimum zones in the eastern tropical Atlantic and Pacific oceans, *Prog. Oceanogr.*, *77*, 331–350, doi:10.1016/j.pocean.2007.05.009.

Key, R. M., et al. (2004), A global ocean carbon climatology: Results from GLODAP, *Global Biogeochem. Cycles*, *18*, GB4031, doi:10.1029/2004GB002247.

LaVigne, M., T. M. Hill, H. J. Spero, and T. P. Guilderson (2011), Bamboo coral Ba/Ca: Calibration of a new deep ocean refractory nutrient proxy, *Earth Planet. Sci. Lett.*, *312*, 506–515, doi:10.1016/j.epsl.2011.10.013.

LaVigne, M., A. G. Grottoli, J. E. Palardy, and R. M. Sherrell (2016), Multi-colony calibrations of coral Ba/Ca with a contemporaneous *in situ* seawater barium record, *Geochim. Cosmochim. Acta*, *179*, 203–216, doi:10.1016/j.gca.2015.12.038.

Lynn, R. J., and J. J. Simpson (1987), The California current system: The seasonal variability of its physical characteristics, *J. Geophys. Res.*, *92*, 12947–12966, doi:10.1029/JC092ic12p12947.

McQuatters-Gollop, A., et al. (2011), Is there a decline in marine phytoplankton?, *Nature*, *472*, E6–E7, doi:10.1038/nature09950.

Moffitt, S., R. Moffitt, W. Sauthoff, C. Davis, K. Hewett, and T. Hill (2015), Paleoceanographic insights on recent oxygen minimum zone expansion: Lessons for modern oceanography, *PLoS One*, *10*(1), doi:10.1371/journal.pone.0115246.

Noe, S. U., and W. C. Dullo (2006), Skeletal morphogenesis and growth modes of modern and fossil deep-water isidid gorgonians (Octocorallia) in the West Pacific (New Zealand and Sea of Okhotsk), *Coral Reefs*, *25*, 303–320, doi:10.1007/s00338-006-0095-8.

Raddatz, J., A. Rüggeberg, V. Liebetrau, A. Foubert, E. Hathorne, J. Fietzke, A. Eisenhauer, and W.-C. Dullo (2014), Environmental boundary conditions of cold-water coral mound growth over the last 3 million years in the Porcupine Seabight, Northeast Atlantic, *Deep-Sea Res. II*, *99*, 227–236, doi:10.1016/j.dsr2.2013.06.009.

Reid, J. L. (1965), *Intermediate Waters of the Pacific Ocean*, p. 85, Johns Hopkins Oceanographic Studies, Baltimore, Md.

Risk, M. J., J. M. Heikoop, M. G. Snow, and R. Beukens (2002), Lifespans and growth patterns of two deep-sea corals: *Primnoa resedaeformis* and *Desmophyllum cristagalli*, *Hydrobiologia*, *471*, 125–131.

Roark, B., T. Guilderson, S. Flood-Page, and R. Dunbar (2005), Radiocarbon-based ages and growth rates of bamboo corals from the Gulf of Alaska, *Geophys. Res. Lett.*, *32*, L04606, doi:10.1029/2004GL021919.

Roemmich, D., and J. McGowan (1995), Climate warming and the decline of zooplankton in the California Current, *Science*, *267*, 1324–1326, doi:10.1126/science.267.5202.1324.

Saenger, C., and J. M. Watkins (2016), A refined method for calculating paleotemperatures from linear correlations in bamboo coral carbon and oxygen isotopes, *Paleoceanography*, *31*, 789–799, doi:10.1002/2016PA002931.

Schlitzer, R. (2016), Ocean data view. [Available at http://odv.awi.de.]

Sinclair, D., L. Kinsley, and M. McCulloch (1998), High resolution analysis of trace elements in corals by laser ablation ICP-MS, *Geochim. Cosmochim. Acta*, *62*(11), 1889–1901, doi:10.1016/S0016-7037(98)00112-4.

Sinclair, D., B. Williams, G. Allard, B. Ghaleb, S. Fallon, S. W. Ross, and M. Risk (2011), Reproducibility of trace element profiles in a specimen of the deep-water bamboo coral Keratoisis sp, *Geochim. Cosmochim. Acta*, *75*(18), 5101–5121, doi:10.1016/j.gca.2011.05.012.

Snyder, M., L. Sloan, N. Diffenbaugh, and J. Bell (2003), Future climate change and upwelling in the California Current, *Geophys. Res. Lett.*, *30*(15), 1823, doi:10.1029/2003GL017647.

Strzepek, K. M., R. E. Thresher, A. T. Revill, C. I. Smith, A. F. Komugabe, and S. F. Fallon (2014), Preservation effects on the isotopic and elemental composition of skeletal structures in the deep-sea bamboo coral *Lepidisis* spp. (Isididae), *Deep Sea Res., II*, *99*, 199–206, doi:10.1016/j.dsr2.2013.07.010.

Sylvester, P. (2008), Matrix effects in laser ablation ICP-MS, in *Laser Ablation-ICP-MS in the Earth Sciences: Current Practices and Outstanding Issues*, *Mineralogical Association of Canada Short Course Series*, vol. 40, edited by R. Raeside, pp. 67–78, Vancouver, B. C.

Talley, L. D. (2008), Freshwater transport estimates and the global overturning circulation: Shallow, deep and throughflow components, *Prog. Oceanogr.*, *78*(4), 257–303.

Thresher, R. E., C. M. MacRae, N. C. Wilso, and S. Fallon (2009), Feasibility of age determination of deep-water bamboo corals (Gorgonacea; Isididae) from annual cycles in skeletal composition, *Deep Sea Res., Part I*, *56*, 442–449, doi:10.1016/j.dsr.2008.10.003.

Thresher, R. E., N. C. Wilson, C. M. Macrae, and H. Neil (2010), Temperature effects on the calcite skeletal composition of deep-water gorgonians (Isididae), *Geochim. Cosmochim. Acta*, *74*(16), 4655–4670, doi:10.1016/j.gca.2010.05.024.

Thresher, R. E., S. J. Fallon, and A. T. Townsend (2016), A "core-top" screen for trace element proxies of environmental conditions and growth rates in the calcite skeletons of bamboo corals (Isididae), *Geochim. Cosmochim. Acta*, *193*, 75–99, doi:10.1016/j.gca.2016.07.033.

Tracey, D. M., H. Neil, P. Marriott, A. H. Andrews, G. M. Cailliet, and J. A. Sanchez (2007), Age and growth of two genera of deep-sea bamboo corals (family Isididae) in New Zealand waters, *Bull. Mar. Sci.*, *81*, 393–408, doi:10.3354/meps08307.

Van Scoy, K., and E. R. M. Druffel (1993), Ventilation and transport of thermocline and inter- mediate waters in the northeast Pacific during recent El Niños, *J. Geophys. Res.*, *98*, 18,083–18,088, doi:10.1029/93JC01797.

Wolgemuth, K. (1970), Barium analyses from the first GEOSECS test cruise, *J. Geophys. Res.*, *75*, 7686–7687, doi:10.1029/JC075i036p07686.